Assessing Potato Yellow Vein Virus (PYVV) infection using remotely sensed data and multifractal analysis

P. Chávez[1], P. Zorogastúa[1], C. Chuquillanqui[2], L.F. Salazar[2], C.Yarlequé[1], A. Posadas[1], O. Piro[3], J. Flexas[4], V. Mares[1], **R. Quiroz**[1]

[1] International Potato Center (CIP). Production Systems & the Environment Division.
[2] International Potato Center (CIP). Integrated Crop Management Division.
[3] University of Balearic Islands (UIB). Research Group on Plants under Mediterranean Conditions. Palma de Mallorca, Spain.
[4] University of Balearic Islands (UIB). Physics Department. Palma de Mallorca, Spain.
perla.chavez@uib.es, p.zorogastua@cgiar.org; c.chuquillanqui@cgiar.org; lsalazar@agdia.com; c.yarleque@cgiar.org; a.posadas@cgiar.org; piro@ifisc.uib.es; jaume.flexas@uib.es; v.mares@cgiar.org; r.quiroz@cgiar.org

Abstract

Potato Yellow Vein Virus (PYVV) reduces potato production in South America. Visual crop monitoring is a standard practice but the disease is generally detected after significant damage has occurred to photosynthetic tissues. Thus, a method for monitoring crop condition at different spatial scales to detect the disease before yields are severely affected is needed. Remotely sensed multispectral reflectance, based on the reflectivity and propagation of light inside plant tissues, was tested for the detection of PYVV infection in potato plants grown indoors. Visual assessment of symptoms in both virus-infected and healthy virus-free plants was compared to monitoring based on spectroradiometry and multispectral photographic images of the plants. Observed disturbances in light reflection by vascular tissues in infected plants, as well as spectral Vegetation Indices such as NDVI, SAVI, and IPVI, provided early detection of viral infection, long before symptoms of chlorosis were visually detected. To improve the earliness of detection, the raw remote sensing data from two subsequent experiments was further processed by multifractal analysis, a mathematical tool that addresses the scale dependency and variability of geophysical variables. Results showed that early diagnosis of PYVV infection was improved, providing the earliest detection of infection ever reported. For the first data set, the infection was evidenced 12 days after inoculation (23 days before the visual assessment did see the symptoms). For the second data set, our analysis denoted the disease 4 days after inoculation (33 days prior to the appearance of symptoms).

Introduction

Potato Yellow Vein Virus (PYVV), a Crinivirus of the Closteroviridae family (Salazar, 1998; Salazar *et al.*, 2000), is considered a threat to potato production in South America (Saldarriaga *et al.*, 1988; Salazar, 1998). PYVV is transmitted semi-persistently by 1) the whitefly *Trialeurodes vaporariorum* Westwood (Diptera, Sternorrhyncha, Aleyrodidae) (Díaz *et al.*, 1990; Tamayo and Navarro, 1984; Salazar, 1998; Salazar *et al.,* 2000), 2) tuber seed (Díaz *et al.*, 1990; Salazar, 1998) and 3) by aboveground and underground stem-grafts (Salazar, 1998). The virus does not affect the size and morphology of plants; the typical yellowing of the veins appears between 30 and 40 days after infection, when stems and leaves are already formed (Saldarriaga *et al.*, 1988). Research carried out on sugar beet (*Beta vulgaris*) also infected with a closteroviridae, the Beet Yellow Virus (BYV), showed damage in the photosynthetic mechanism of plants resulting in the reduction of net photosynthesis (Clover *et al.*, 1999). One effect of the virus was the reduction of stomatal conductance, and a 50% reduction of the splitting of water in isolated chloroplasts (Spikes and Stout, 1955) with thylakoidal membrane damage (Baker and Horton, 1988; Salazar, 1998). Similar effects have been observed with PYVV in potatoes by Saldarriaga *et al.* (1988). Unpublished research at CIP shows that PYVV does infect the phloem cells and prevents the flow of carbohydrates, reducing yields drastically.

PYVV infections are not evenly distributed across the field but they may occur in patches in current-season infections. A most widely used practice in the control of PYVV infection is the visual determination and manual elimination or roguing of infected plants and the spraying of pesticides over the whole stand at different times during the cultivation cycle, for the control of vectors. However, the use of pesticides increases costs and pesticide residue levels in agricultural products and soils, and contributes to ground water contamination.

Furthermore, indiscriminate use of pesticides could eliminate natural biological control agents, thus increasing pest-insect populations, such as *Trialeurodes vaporariorum*. For effective disease control, early identification of infection patches in the field is required, allowing for the eradication of infected plants and avoiding the spread of disease (Agrios, 1997).

The multispectral analysis is based on the reflectivity and propagation of solar radiation from and within plant canopies and tissues, where a fraction is absorbed and other reflected in all directions (Gilabert *et al.*, 1997). Reflectivity is linked to the biochemical and structural components of the plant, such as chlorophyll, water, proteins and cell wall materials (Gamon, 1992; Ritchie, 2003), which are affected by diseases, resulting in differences in the spectral signature of healthy and stressed plants.

The present work was aimed at 1) assessing the usefulness of remotely sensed multispectral reflectance imagery and spectroradiometry to determine PYVV infection in potatoes, before symptoms become visually perceptible, and 2) assessing the usefulness of applying multifractal analysis and the wavelet transform to remotely sensed multispectral imagery and spectral-radiometrical data, to enhance their precision and earliness in detecting PYVV infection in plants. Multifractal theory permits the characterization of complex phenomena for both temporal and spatial variations. An important property of the multifractal parameters is that they are scale invariant (Schertzer and Lovejoy, 1989), which means that the information they provide are constant across different scales, allowing for a valid extrapolation up and down scales. This property is particularly relevant in the work herewith reported, as it confers robustness and consistency to the observed results. Thus, it was hypothesized that applying multifractal analysis to remotely sensed multispectral data would improve the diagnostic capabilities of multispectral reflectance imagery and spectroradiometry to determine PYVV infection in potatoes.

Materials and methods

Plant material and treatments

In the first stage of research, three experiments conducted under a split-plot in time design with inoculated and control treatments in the main plot, and time measurements as sub-plots, were carried out indoors in Lima, Peru, from July to November 2004. A total of 27 potato plants, cv. Costanera, six infected with PYVV and 3 virus-free as control, comprised each repetition. In the second stage of research, two indoors experiments were carried out in Lima, Peru, from May to September 2007. Twenty plants of potato cv. Yungay per experiment, divided in Control and virus-inoculated PYVV plants comprised each repetition.

In both stages (2004 and 2007), plants were initially germinated in a nursery and then transplanted into individual 6 litres pots containing a mixture of compost (10%), vegetal soil (70%) and perlite stone (20%) as substrate. Then, the PYVV infection was induced through lateral grafting in PYVVi plants some 2 weeks after emergence. The environmental conditions (temperature, relative humidity, light) and management were similar for infected and control plants. The pots were located under an insects-free net house and irrigated to maintain the soil at field capacity.

Data collection

In both 2004 and 2007, a comparative visual assessment of both PYVV-infected plants (PYVVi) and healthy virus-free plants was continuously conducted to monitor the development of disease symptoms in the former. At the same time, multispectral photographic images of the same plants were recorded during their growth and development cycle, using an Agricultural Digital Camera (ADC Dycam, Inc., red and near infrared sensors, in the first stage; Tetracam Inc., red, green and NIR sensors, second stage). The camera was placed 0.60 m above the photographed plants. Pictures were taken at the same time of day every 4-5 days. The images were analyzed through the freeware software Briv32 (Band Rationing Image Viewer, Tetracam Inc. USA) to obtain the spectral vegetation indices (SVI): the normalized difference vegetation index (NDVI = $(R_{NIR}-R_{red})/(R_{NIR}+R_{red})$, R=reflectance, ranging from –1 to +1) that track changes in chlorophyll concentration (Dobrowski *et al.*, 2005); the soil adjusted vegetation index (SAVI = $[(R_{NIR}-R_{red})/(R_{NIR}+R_{red}+L)*(1+L)]$, where L ranges from 0 to 1), proposed as a soil-line vegetation index to reduce the background contribution (Huete, 1988); and the infrared percentage vegetation index (IPVI = $R_{NIR}/(R_{NIR}+R_{red})$), a ratio-based index that holds a limited range with no negative values (0<IPVI<1), whose main disadvantage is its sensitivity to atmospheric noise (Crippen, 1990). These SVIs had proved to be good indicators of infection by PYVV in potato (Chávez *et al.*, 2009a).

Light reflectance from the individual plants was recorded during approximately 40 days after the virus inoculation, until the disease's symptoms were visually perceptible. During the first stage, measurements of light reflectance were taken weekly using a Li-Cor 1800 spectroradiometer (Li-Cor Inc., Nebraska, USA) covering the 350–850 nm wavelength region. The aperture angle of the fore optics of the spectroradiometer was 180° that became 60º because of its built-in cosine corrector, so the instantaneous field of view (IFOV) was 0.2m diameter (distance from canopy was 0.2m). Measurements were taken from nadir. In the second stage, a computer assisted ASD Fieldspec Pro spectroradiometer (Analytical Spectral Devices Inc., Colorado, U.S.A.), covering the 325–1075 nm wavelength region, was used for data recording. 2007 comprised a first experiment with an aperture angle of the fore optics of 25º, and a second one using a collimator to reduce the aperture angle to 1º. Measurements were taken from nadir at a distance of 30 cm from the plant canopy, resulting in a IFOV of 13cm and 0.52cm diameter, respectively, first and second experiment. A white teflon and a Spectralon® panel were used in 2004 an 2007, respectively, for converting the reflected radiation into relative reflectance values. In the 2007's experiments, measurements were taken every 2 - 3 days with the sun at 30º of zenith angle throughout the observational period.

Data processing

The reflectance spectra data obtained in 2004 were assessed by dividing the spectrum measured into the main four sectors (blue, green, red and near infrared) for calculating the percentage of reflectance against time. First- and second-order derivatives were also calculated from the spectroradiometric measurements through the IDL 6.1 software (Research Systems Inc.), as well as for the values of the vegetation indices calculated from the spectral photography. A similar assessment of reflectance spectra was carried out with the data from the second stage (2007) to contrast the information it provided against the results of the wavelet-multifractal analysis of the same data.

A software that describe the canonical method of wavelet multifractal modulus maximum, originally implemented by McAteer *et al.* (2007) to run it in IDL6.2 for Linux, was modified to analyze our reflectance spectrum data. The methodology described by Arneodo *et al.* (1988) was followed and adapted to run in IDL6.3 for Windows. The reflectance data obtained in 2007 experiments were processed with the Continuous Wavelet Transform (CWT) and the wavelet transform modulus maxima (WTMM) method using as mother wavelet analyser the second derivative of the Gaussian function (Mexican hat). For more details on the subject, see the papers by Arneodo *et al.* (1995), McAteer *et al.*, (2007) and Chávez *et al.* (2009b).

Data pre-processing for multifractal analysis

The pre-processing consisted of two steps. In the first one a background correction was required to account for changes in the signal due to both measurement errors and natural changes in the atmosphere while measuring all the plants within a sampling date. The background correction was performed by adjusting the measured response (G) of individual plant signals to a reference response through fitting a linear regression (Equation 1; Yarlequé, 2009). In the second step, the anomalies over moving averages of 41 wavelengths (see equations 2 and 3) were calculated. Anomalies reduce the signal to noise ratio thus making small fluctuations in the physiology of the plant more perceptible by the analyses.

Background correction: $$S(t_i) = A.G(t_i) + B \qquad (1)$$

Where, $A = \frac{(G_{max} - G_{min})}{(G_{Total\ max} - G_{Total\ min})}$. In this equation the numerator is measured from every plant, while the denominator is the difference between maximum and minimum values of recorded reflectance among all the plants (Ctrl and PYVVi) in one determined date; and G and S are the measured and estimated passive reflectance according to t wavelength (nm), respectively. Finally, $B = G_{min} - A.G_{Total\ min} = G_{max} - A.G_{Total\ max}$

Moving average: $$\hat{S}(t_i) = \sum_{k=i-20}^{i+20} \frac{S(t_k)}{41}, \quad , \qquad (2)$$

Anomalies: $$S'(ti) = S(ti) - \hat{S}(ti) . \qquad (3)$$

Statistical analyses

Differences between means of infected and healthy plants were revealed by split plot in time design with repeated measurement analyses and independent samples test, using the SAS software package (SAS, North Carolina, U.S.A.). The GLM method described by Wolfinger and Chang (1998) was used for the repeated measurement analyses.

Results and discussion

Reflectance measurements

In the 2004 experiments, a distinct reflectance pattern from infected plants was evident 23 days after inoculation (dai) (Figure 1) through changes in reflectance in the blue region (450–495 nm) ($P<0.01$). Reflectance in the green region (495–570 nm) provided the same response at a similar time after infection, but it seems to be less reliable ($P<0.05$). Responses in the red region (620–750 nm) presented more noise and no differences between infected and healthy plants were detected ($P>0.05$). As to the NIR region (> 750 nm) differences in reflectance could be detected as early as 11 dai ($P<0.05$). However, the responses in the NIR were highly variable in time, making it an unreliable indicator of the presence of symptoms.

In 2007, it was impossible to determine the infection through the direct observation of the reflectance data obtained through a 25º solid-angle sensor's aperture. However, when the data was pre-processed prior to multifractal analysis, differences between treatments were detected ($P<0.05$) from the 12th dai (i.e. 23 days before symptoms became visible (Figure 2) as visual symptoms of viral infection in PYVVi plants were noticed from the 36th dai onwards). From the 21st to the 26th dai, the singularity spectrums of both treatments were transiently similar, suggesting a recovery of the PYVV infected plants, but differences again became significant from 28th dai onwards.

The second experiment of 2007 was designed to test whether a higher precision of the IFOV would reveal changes directly from recorded data, thus the sensor aperture of fore-optics of the spectroradiometer was adjusted to 1º by means of a collimator. In this instance, the multispectral reflectance revealed that PYVVi and Ctrl plants originated very distinct spectra that were easily noticeable, well before symptoms of PYVV infection were visually observed, which occurred 37 days after infection. Moreover, the multifractal analysis of both raw and pre-processed data strongly enhanced the evidence of such spectral differences making them noticeable even earlier than in the previous experiment, the 4th dai –i.e. 33 days before the symptoms were visible (Figure 3). As observed before, an apparent unexpected transient recovery of PYVVi plants occurred from the 10th to the 15th dai.

Earliness of PYVVi diagnosis was sharper and faster in the second experiment 2007 as a consequence of differences in the solid angle of sensor aperture producing a different size of their IFOV. As described above, the first experiment had a fore-optic aperture of 25º that provided an IFOV of 13cm of diameter, whereas in the second experiment the aperture was 1º and the IFOV diameter was 0,52cm. The smaller sensed area gave a sharper measurement as the incoming scattering was close to zero. In contrast, in the first experiment, the 25º of fore-optic aperture permitted a higher scattering influence from the surrounding area, producing a less sharp measurement.

Visible and Near-Infrared reflectance

Dividing the spectra into main regions for the 2007 experiments, a distinct reflectance pattern from infected plants was evident for several wavelengths at 25 dai (25º of sensor aperture) ($P<0.05$), and 23 dai (1º of sensor aperture) ($P<0.05$). The blue region (450-495 nm) showed the most robust statistical response. Reflectance in the green region (495–570 nm) seemed to be a less reliable indicator. Responses in the red region (620–750 nm) presented more noise. Near-infrared reflectance were highly variable in time (data not shown), then NIR would be an unreliable indicator of the infection, confirming the results obtained by the multifractal analysis described in the section above. Our results suggest that multifractal analysis of the entire visible region or the complete reflectance spectrum (visible and NIR) is required to obtain reliable information about the PYVV infection in potato plants. They also confirmed the accuracy of this methodology as obtained by Chávez *et al.* (2009) in which telltale anomalies in reflectance were detected some 14 days before symptoms were visible. In our previous work we used a sensor with an aperture of 180º -that became 60º due to its built-in cosine corrector-

without significant changes in the results-, so it would indicate that with sensor aperture ≥ 25º there might be no substantial changes in the measure.

Spectral vegetation indices

Dobrowsky *et al.*, (2005) pointed out that the majority of vegetation indices (SVI) are not sensitive to rapid changes in plant photosynthetic status caused by environmental stressors, due to most SVI have not direct link to photosynthetic functioning. Nevertheless, our results did show (Figure 4) a good diagnosis capability of NDVI, SAVI and IPVI for viral infection in potato plants, suggesting that damage to the photosynthetic tissues produced by the virus infection are rapidly reflected in the components of the SVI. In fact, the SVI's calculated from the multispectral images captured by the 3 bands (red, green and NIR) agricultural camera did show differences around 5 days before the diagnosis obtained in the previous work, which used a 2 bands (red and NIR) camera.

Recovery period

The recovery of infected plants could be explained by the adaptive defense mechanisms of plants specially targeted on avoiding viral infections, called RNA silencing. The plant perceives information from the infecting virus genome and produces a specific defensive response for that genome (Argerter, 1999). The silencing RNA mechanism mediates the post- transcriptional repression of the target gene expression and represses the proliferation and expression of different invading nucleic acids, such as those carried by viruses, viroids, transposons or transgenes, as well as regulates the gene expression (Baulcombe, 2004). The silencing response may not be limited to the plant cell the virus is actively infecting but extends into newly dividing cells at the plant's growing points, and enables plant cells far removed from the initial infection site to be prepared when viruses get to them (Argerter, 1999). Young plants can exert more resistance to viral infection and endogenously expressed viral transcripts (Siddiqui, 2007), so it could explain the temporary recovery of PYVVi plants, since plants at this stage were juveniles. Later on, the barrier of silencing RNA was overwhelmed by the infection and symptoms developed. Ding (2000) and Baulcombe (2008, personal communication), explained that the recovery is cyclical, but, after a period the virus accumulates to higher levels and the disease overcomes the plant.

Conclusions

Early diagnosis of PYVV infection in potato plants was improved by applying multifractal analysis to the primary remotely sensed multispectral reflectance data recorded in 2007, allowing for the earliest detection of infection ever reported: 12 dai –i.e. 23 days prior to the appearance of visual symptoms –and 4 dai –i.e. 33 days before visual symptoms appeared- (1º of sensor aperture).

Multifractal analysis of pre-processed data was very effective and sharper than multifractal analysis of raw data obtained through a fore optic sensor aperture of 25º. It appears that pre-processing is necessary when the solid angle aperture sensor is 25º, but it is not imperative when the solid angle aperture sensor is 1º, due to the precision of focus. So, pre-processing (background correction and the use of anomalies) increases the signal to noise ratio thus increasing the likelihood of earlier detection of differences

The main advantages of multifractal analysis lay on the earliness of diagnosis of PYVV infection in plants and the statistical accuracy of results. This is due to the amplification of differences, which is an intrinsic feature of the methodology. The sensitivity with this processing methodology is such that differences prior to the fast and interim recovery period can be detected.

The spectral vegetation indices NDVI, SAVI and IPVI confirmed their usefulness in accurately evidencing the infection caused by PYVV, and the use of a three bands camera improved the earliness of prediction in 5 days compared to the diagnosis based on the use of a two bands camera as reported before. Nonetheless, with SVI's the differences are evident after the recovery period.

The methodology based on dividing the multispectral reflectance spectrum into the main wavelength regions (blue, green, read, NIR), has confirmed its accuracy in diagnosing the PYVV infection, 25 and 23 days after the virus inoculation.

Acknowledgments

Support for this work was provided by the International Foundation for Science (IFS Grant 4068/-I), the Production Systems and the Environment Division of the International Potato Center (CIP) and the Agencia Española para la Cooperación Internacional (AECID). The authors thank to Christopher Clark and Arnauld Thiry, for comments and helpful criticism of earlier drafts of this paper. Jimena Bazoalto from CIP contributed to data processing. Thanks to Luciano Ponce, Hugo Espinoza, Richard Uribe, and Luis Silva from CIP, for the logistical support, and to McAteer for kindly share your wavelet-multifractal algorithm, and to Salomon Helfgott and Vicente Rázuri from La Molina University for their good advices.

References

Agrios, G.N. 1997. Plant Pathology, fourth edition, Academic Press. New York.

Argerter, M. 1999. Plant viruses discover how to overcome gene silencing. Universe Magazine. Washington State University, U.S.A. http://www.wsu.edu/NIS/Universe/virus.htm

Arneodo, A.; Grasseau, G.; Holschneider, M. 1988. Wavelet transform of multifractals. Phys. Rev. Lett. 61(20), 2281-2284.

Arneodo, A.; Bacry, E.; Graves, P.V.; Muzzy, J.F. 1995. Characterizing long-range correlations in DNA sequences from wavelet analysis. Phys. Rev. Lett., 74(16), 3293-3296.

Baker, N.R., Horton, P., 1988. Chlorophyll fluorescence quenching during photo inhibition. In: Kyle, D.J., Osmond, C.B., and Arntzen, C.J. (eds). Photo inhibition. Amsterdam, Netherlands: Elsevier, 145-168.

Baulcombe, D. 2004. RNA silencing in plants. Nature, 431(7006), 356-363.

Chávez, P.; Zorogastúa, P.; Chuquillanqui, C.; Salazar, L.F.; Mares, V.; Quiroz, R. 2009(a). Assessing potato yellow vein virus (PYVV) infection using remotely sensed data. International Journal of Pest Management, 55(3), 251-256.

Chávez, P., Yarlequé, C., Piro, O., Posadas, A., Mares, V., Loayza, H., Chuquillanqui, C., Zorogastúa, P., Flexas, J., Quiroz, R. 2009(b). Applying multifractal analysis to remotely sensed data for assessing PYVV infection in potato (*Solanum tuberosum* L.) crops. Remote Sensing Journal. Under revision.

Clover, G.R.G., Azam-Ali, S.N., Jaggard, K.W., Smith, H.G. 1999. The effects of beet yellows virus on the growth and physiology of sugar beet (*Beta vulgaris*). Plant Pathology, 48(1), 129-138.

Crippen, R.E. 1990. Calculating the vegetation index faster. Rem. Sens. of Environ., 34(1), 71-73.

Díaz, M.C., Pulgarín, J.M., Saldarriaga, A. 1990. Relaciones insecto-patógeno en el problema del amarillamiento de venas en papa. Revista Colombiana de Entomología, 16(2), 3-14.

Ding, S.W. 2000. RNA Silencing. Curr Opin Biotechnol., 11(2), 152-156.

Dobrowski, S.Z.; Pushnik, J.C.; Zarco-Tejada, P.J.; Ustin, S.L. 2005. Simple reflectance indices track heat steady-state chlorophyll fluorescence at the canopy scale. Rem. Sens. of Environ., 97(3), 403-414.

Gamon, J.A.; Peñuelas, J.; Field, C.B. 1992. A narrow waveband spectral index that tracks diurnal changes in photosynthetic efficiency. Rem. Sens. of Environ., 41(1), 35-44.

Gilabert, M.A.; García-Haro, F.J.; González Piqueras, J. 1997. Acerca de los índices de vegetación. Revista de Teledetección, 8, 1-10.

Huete, A.R. 1988. A soil-adjusted vegetation index (SAVI). Remote Sensing of Environment, 25(3), 295-309.

McAteer, R T.J.; Young, C.A.; Ireland, J.; Gallagher, P.T. 2007. The bursty nature of solar flare x-ray emission. The Astrophysical Journal, 662(1), 691-700.

Ritchie, G.L. 2003. Use of ground-based canopy reflectance to determine radiation capture, nitrogen and water status, and final yield in wheat. Thesis for Magister in Science academic degree, Utah State University, USA.

Schertzer, D.; Lovejoy, S. 1989. Nonlinear variability in geophysics: multifractal analysis and simulation. In: Pietronero, L., (ed.) Fractals: Physical origin and consequences, Plenum: New York, pp 49-79.

Salazar, L. 1998. La enfermedad del amarillamiento de las venas de la papa: Evidencia de la presencia de un virus inusual. Agroenfoque. Perú, 12(85), 24-26.

Salazar, L.F.; Muller, G.; Querci, M.; Zapata, J.L.; Owens, R.A. 2000. Potato yellow vein virus: its host range, distribution in South America and identification as a crinivirus transmitted by *Trialeurodes vaporariorum*. Ann. Appl. Biol. 137(1), 7-19.

Saldarriaga, A., Alvarez, A., Jaramillo, J. 1988. Efecto del amarillamiento de venas transmitido por *Trialeurodes vaporariorum* (Westwood) en papa. Revista Colombiana de Entomología, 14(2), 3-8.

Siddiqui, S.A. 2007. RNA Silencing and its inhibition in transgenic tobacco plants. Thesis. University of Turku, Finland.

Spikes, J.D.; Stout, M. 1955. Photochemical activity of chloroplasts isolated from sugar beets infected with virus yellows. Science Magazine, 122(3165), 375-76.

Tamayo, P.; Navarro, R. 1984. Aumenta la incidencia del virus de amarillamiento de venas de la papa en Antioquia. ASCOLFI Informa (Bogotá) 10, 40-42.

Wolfinger, R.D.; Chang, M. 1998. Comparing the SAS GLM and MIXED Procedures for Repeated Measures, SUGI Proceedings: Cary, NC, USA

Yarlequé, C. 2009. Análisis de campos de biomasa del altiplano usando wavelet y parámetros universales multifractales. Tesis de Licenciatura en Física. Universidad Nacional del Callao, Perú, p 202.

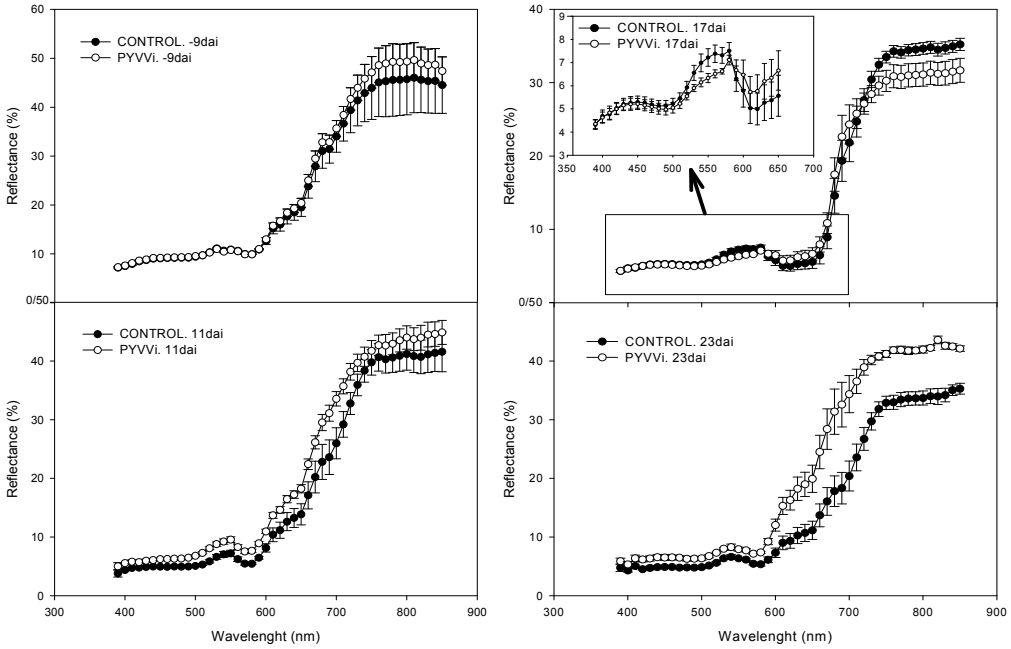

Figure 1. Reflectance of potato plants, 2004, Reflectance differences between treatments were observed from 11 dai onwards

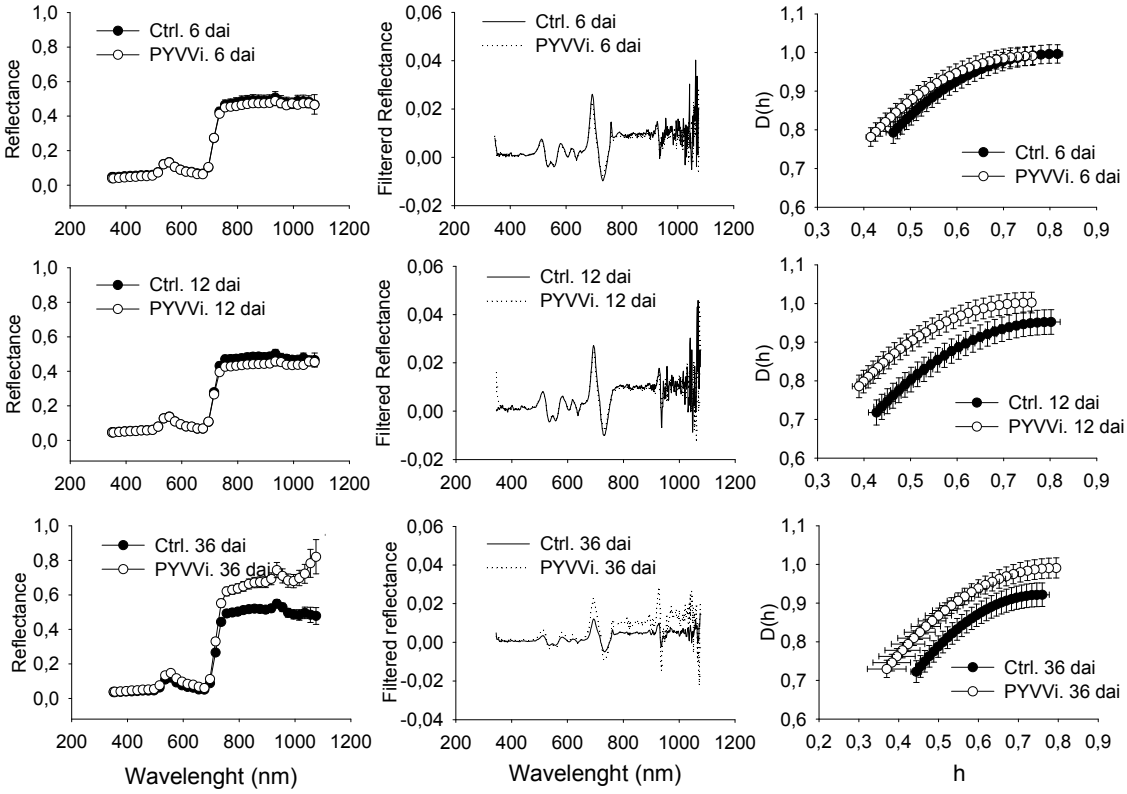

Figure 2. First 2007 experiment, 25º of sensor aperture. Passive reflectance of plants (*left*), the same reflectance after background correction, moving average and anomalies (*centre*), and their correspondent singularity multifractal spectra (*right*).

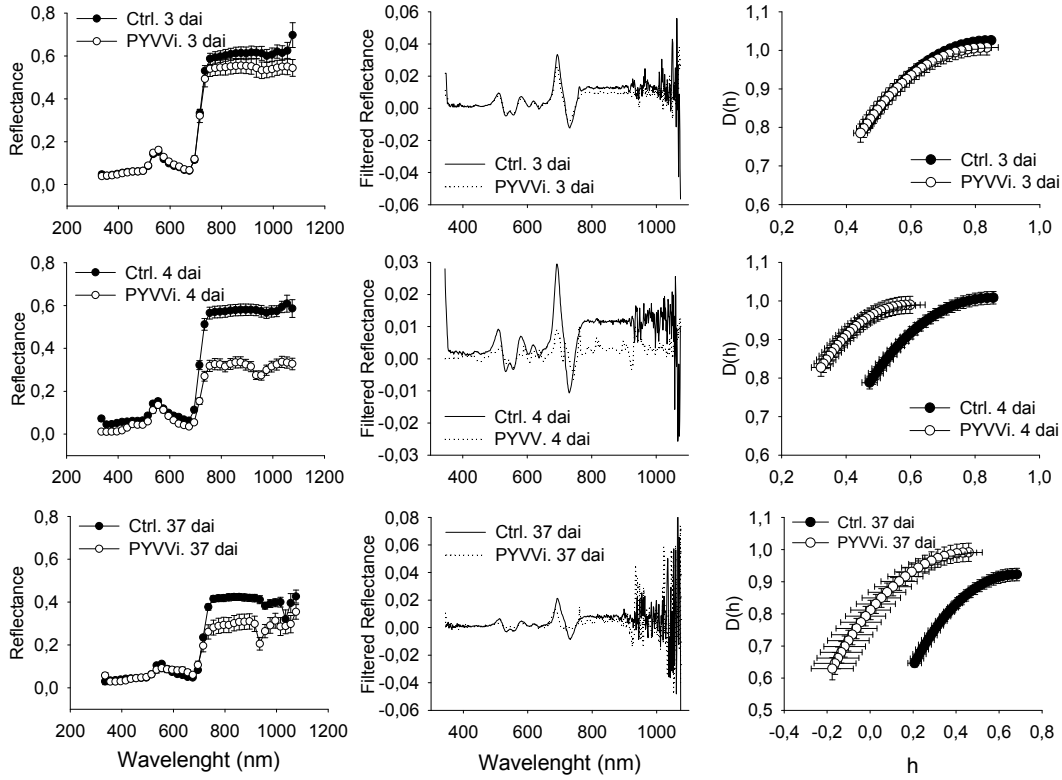

Figure 3. Second 2007 experiment, 1º of sensor aperture. Passive reflectance of plants (*left*), the same reflectance after background correction, moving average and anomalies (*centre*), and their correspondent singularity multifractal spectra (*right*). Multifractal spectrum reveals changes at the 4th dai.

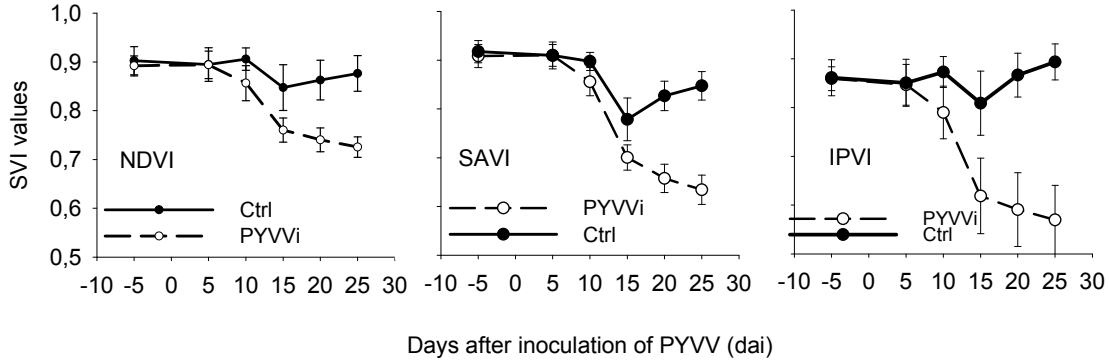

Figure 4. Spectral Vegetation Indices of the second experiment, 2007